Mathematical Biosciences and Engineering

http://www.aimspress.com/journal/MBE

MBE, 19(2): 1128–1153.
DOI: 10.3934/mbe.2022052
Received: 18 October 2021
Accepted: 24 November 2021
Published: 30 November 2021

Research article

Photovoltaic models parameter estimation via an enhanced Rao-1 algorithm

Junhua Ku[1], **Shuijia Li**[2] **and Wenyin Gong**[2,*]

[1] School of Science, Qiongtai Normal University, Haikou, 571127, China
[2] School of Computer Science, China University of Geosciences, Wuhan 430074, China

* **Correspondence:** Email: wygong@cug.edu.cn; Tel: +86-27-67883716.

Abstract: The accuracy of unknown parameters determines the accuracy of photovoltaic (PV) models that occupy an important position in the PV power generation system. Due to the complexity of the equation equivalent of PV models, estimating the parameters of the PV model is still an arduous task. In order to accurately and reliably estimate the unknown parameters in PV models, in this paper, an enhanced Rao-1 algorithm is proposed. The main point of enhancement lies in i) a repaired evolution operator is presented; ii) to prevent the Rao-1 algorithm from falling into a local optimum, a new evolution operator is developed; iii) in order to enable population size to change adaptively with the evolutionary process, the population size linear reduction strategy is employed. To verify the validity of ERao-1 algorithm, we embark a study on parameter estimation of three different PV models. Experimental results show that the proposed ERao-1 algorithm performs better than existing parameter estimation algorithms in terms of the accuracy and reliability, especially for the double diode model with RMSE 9.8248E-04, three diode model with RMSE 9.8257E-04 for the R.T.C France silicon cell, and 2.4251E-03 for the three diode model of Photowatt- PWP201 cell. In addition, the fitting curve of the simulated data and the measured data also shows the accuracy of the estimated parameters.

Keywords: Parameter estimation; photovoltaic model; Rao-1 algorithm; parameter extraction

1. Introduction

Currently, the renewable energy is receiving more and more attention due to its some promising features such as clean, no pollution, and widespread, which is incomparable to traditional energy sources [1]. In general, these are commonly used renewable energy sources such as solar energy, wind energy, nuclear energy, tidal energy, and geothermal energy [2]. Among these energies, the solar energy and wind energy are considered the most promising energy sources, because they can be widely available. Compared with wind energy, solar energy plants are easier to install. With the development of photovoltaic (PV) technology, solar energy has drew more and more attention. For a PV system,

choosing an accurate model is very important, which is of great significance on evaluation of solar cell performance. To this end, three PV models. namely single diode mode (SDM) [3], double diode model (DDM) [4], three diode model (TDM), and its variants on PV module (PVM) [5] are proposed for the PV system. For the SDM and single PVM, it is composed of a photo-generated current source, diode, equivalent series resistance and equivalent parallel resistance. While for the DDM and TDM, different from the former, there are two and three diodes. However, there is no free lunch. These PV models have unknown parameters that need to be estimated. For example, five unknown parameters such as photo-generated current (I_{pg}), diode reverse saturation current (I_{rs}), series resistance (R_{se}), shunt resistance (R_{sh}), and non-physical diode ideality factor (n) need to be identified in the SDM and single PVM. These parameters are critical to PV models, which is helpful for the design and optimization of the solar cell. Therefore, regardless of the PV model used in the PV system, these unknown parameters must be accurately identified. Thus, designing an effective PV parameter estimation algorithm is becoming more and more urgent.

Over the past few years, researchers have come up with various of methods for parameter estimation of PV models. To sum up, three categories such as analytical methods, deterministic methods and heuristic methods can be broadly divided into according to the characteristics of the method. The analytical method is a simple and fast method, which reduces the complexity of the problem by analyzing the equivalent equations of PV models based on some hypothesis. The advantage is that it is simple and does not consume a lot of computing resources. However, the accuracy of this method depends heavily on the correctness of the hypothesis. The deterministic method such as Newton-Raphson method [6] and Lambert W-functions method [7], does not require pre-assumptions, but it needs to provide an initial guess in advance. However, this method is susceptible to the initial estimates, and if the initial estimates are not good enough, it is easy to obtain the estimated unknown parameters with low precision. In addition, this method has a strict requirement on the optimization objective that should be continuous, convex, and differentiable [5]. Unfortunately, these requirements are often difficult to meet for the PV models equivalent equations. In order to alleviate the shortcomings of the above methods, researchers have employed and developed many heuristic methods to estimate the unknown parameters of PV models. The heuristic method is a kind of trial-and-error based method inspired by natural environment phenomena. This approach is simple to implement, and more importantly, it does not require any assumptions, but also does not depend on the characteristics of the problem. In addition, it has no additional requirements for the optimization objective. Therefore, in recent years, more and more heuristic methods and their improved variants such as simulated annealing algorithm (SA) [8], pattern search (PS) [9], particle swarm optimization (PSO) [10], differential evolution (DE) [11, 12], hybrid teaching-learning-based optimization and differential evolution (ATLDE) [13], whale optimization algorithm (WOA) [14], generalized oppositional teaching learning based optimization (GOTLBO) [15], improved JAYA algorithm (IJAYA) [16], multiple learning backtracking search algorithm (MLBSA) [17], hybrid teaching-learning-based optimization and artificial bee colony (TLABC) [18], performance-guide JAYA algorithm (PGJAYA) [19], improved teaching learning based optimization (ITLBO) [20], and so on, have been developed to identify the unknown parameters in PV models. Figure 1 shows an overview survey on some recent and popular algorithms for PV model parameter estimation, where the PSO, DE, TLBO, JAYA, and hybird methods are the most used. In addition, many new heuristic methods are developed to solve this problem in recent years. There is no doubt that these methods have achieved better results than previous ones. However,

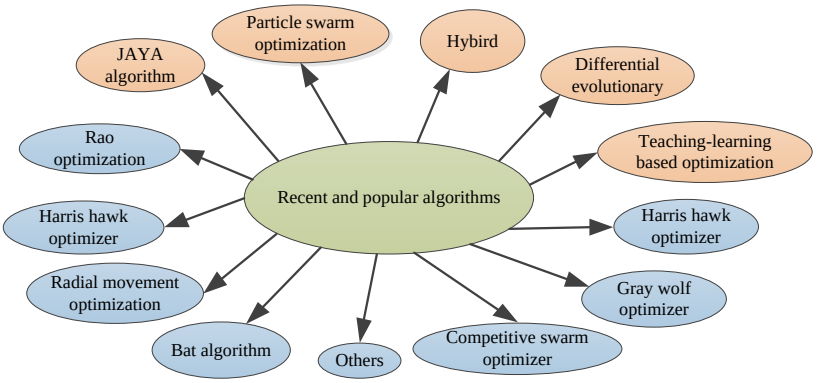

Figure 1. An overview survey on some recent and popular algorithms for PV model parameter estimation.

the performance of most algorithms is affected by their arithmetic parameters, which makes it difficult for users to give a suitable parameter value for different problems. When solving a new problem, users need to do a lot of pre-experiments to get a suitable parameter value, which greatly increases the computational burden.

Rao-1 algorithm is a simple and parameter-free heuristic method, which is proposed for solving optimization problems with and without constraints [21]. Different from some of the algorithms mentioned earlier, on the one hand, Rao-1 algorithm has no additional control parameter except the common parameter known as the population size. For example, the inertia weight and acceleration coefficients are need to set in PSO. In DE, the scaling factor and crossover rate should be given according to different problems. Benefit from parameter-free, Rao-1 algorithm can relieve the burden of user choosing an appropriate parameter value. On the other hand, the Rao-1 algorithm only has one evolution operator when solving optimization problems, which makes it easy to implement and can quickly provide an optimal solution. Therefore, the Rao-1 algorithm has been applied for engineering optimization problems such as mechanical system optimization [22], reduced-order active disturbance rejection control [23], PV models parameter estimation [24, 25], etc. As can be observed, the Rao-1 algorithm also has been applied for PV models optimization. However, the results in [24] show that it is easy to fall into local optimum. While in [25], it needs a lot of computing resources to obtain satisfactory results. Thus, a simple and effective improved Rao-1 algorithm becomes urgent.

Inspired by the promising features of Rao-1 algorithm, in this paper, for the purpose of accurately and reliably estimating the unknown parameters in PV models, an enhanced Rao-1 algorithm referred as ERao-1 is proposed. In ERao-1, firstly, a repaired evolution operator is proposed to reduce the randomness in original evolution operator of Rao-1 algorithm; secondly, a new evolution operator is developed to prevent the Rao-1 algorithm from falling into a local optimum; thirdly, the population size linear reduction strategy is introduced to enable population size to change adaptively with the evolutionary process. In order to prove the validity of ERao-1 algorithm, three different PV models such as SDM, DDM, and TDM have been used as the suites. The experimental results demonstrate that ERao-1 algorithm can provide competitive performance in the accuracy and reliability of estimated parameters when comparing with some well-established algorithms.

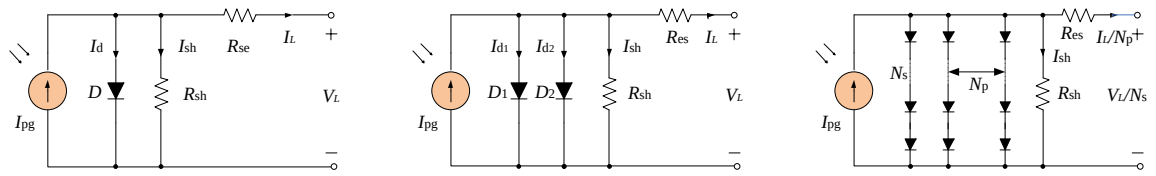

(a) SDM (b) DDM (c) SPVM

Figure 2. Equivalent circuit diagram of various PV models [12].

In summary, the main contributions of this paper can be summarized as follows:

- An enhanced Rao-1 algorithm is developed for parameter estimation of PV models, where a repaired evolution operator is proposed to reduce the randomness in original Rao-1 algorithm.
- Design a new evolution operator to prevent Rao-1 algorithm from falling into local optimum.
- A population size linear reduction strategy is employed to make population size to change adaptively with the evolutionary process.
- The performance of ERao-1 algorithm has been demonstrated by estimating unknown parameters in various PV models.

The structure of the remainder of this paper is organized as follows. The definition of PV models and optimization objectives are described in Section 2. In Section 3, a brief introduction about the original Rao-1 algorithm is described. Section 4 gives the detailed description of the proposed ERao-1 algorithm, and Section 5 reports the experimental results. Lastly, the conclusion of this paper is concluded in Section 6.

2. Definition of PV models and optimization objectives

As described in Introduction, there are three commonly used PV models namely the SDM, DDM, and TDM. In this section, the definition of these PV models and the optimization objective will be introduced.

2.1. SDM

The equivalent circuit diagram of the SDM is given in Figure 2(a), in which there are a photo-generated current source I_{pg}, a diode D, two resistances R_{se} and R_{sh}. According to [26], the output current I_L of this model is calculated as follows:

$$I_L = I_{\mathrm{pg}} - I_{\mathrm{d}} - I_{\mathrm{sh}} \tag{2.1}$$

where I_{d} denotes the diode current, the current of the shunt resistor is represented as I_{sh}. The two currents can be worked out by using the Shockley equation and Kirchhoffs Voltage Law, which is shown as follows

$$I_{\mathrm{d}} = I_{\mathrm{rs}} \left[\exp\left(\frac{(V_L + I_L R_{\mathrm{se}}) \cdot q}{nkT} \right) - 1 \right] \tag{2.2}$$

$$I_{\mathrm{sh}} = \frac{V_L + I_L R_{\mathrm{se}}}{R_{\mathrm{sh}}} \tag{2.3}$$

where V_L denotes the output voltage of the model, I_{rs} represents the diode reverse saturation current, n is the diode ideality factor, q is the a electron charge and its value is $1.60217646 \times 10^{-19}$ C, k is the Boltzmann constant and its value is $1.3806503 \times 10^{-23}$ J/K, while T is the current temperature, which will be converted into Kelvin units when calculating.

On the basis of Eqs. (2.1)-(2.3), the output current I_L can also be written as

$$I_L = I_{\mathrm{pg}} - I_{\mathrm{rs}} \left[\exp\left(\frac{(V_L + I_L R_{\mathrm{se}}) \cdot q}{nkT} \right) - 1 \right] - \frac{V_L + I_L R_{\mathrm{se}}}{R_{\mathrm{sh}}} \tag{2.4}$$

where five unknown parameters I_{pg}, I_{rs}, R_{se}, R_{sh}, and n need to be estimated.

2.2. DDM

Figure 2(b) shows the equivalent circuit of DDM, where there are two diodes D_1 and D_2. For this model, the output current I_L can be formulated as below [26]:

$$I_L = I_{\mathrm{pg}} - I_{\mathrm{d}_1} - I_{\mathrm{d}_2} - I_{\mathrm{sh}} \tag{2.5}$$

where I_{d_1} and I_{d_2} represent the first and second diode currents, respectively, and their formula is shown as follows

$$I_{\mathrm{d}_1} = I_{\mathrm{rs}_1} \left[\exp\left(\frac{(V_L + I_L R_{\mathrm{se}}) \cdot q}{n_1 kT} \right) - 1 \right] \tag{2.6}$$

$$I_{\mathrm{d}_2} = I_{\mathrm{rs}_2} \left[\exp\left(\frac{(V_L + I_L R_{\mathrm{se}}) \cdot q}{n_2 kT} \right) - 1 \right] \tag{2.7}$$

where I_{rs_1} is the diffusion current, I_{sd_2} denotes the saturation current, n_1 is the first ideal coefficient of the non-physical diode, and n_2 denotes the second ideal coefficient of the non-physical diode.

On the basis of Eqs. (2.5)-(2.7), the output current I_L in DDM can be represented as

$$I_L = I_{\mathrm{pg}} - I_{\mathrm{rs}_1} \left[\exp\left(\frac{(V_L + I_L R_{\mathrm{se}}) \cdot q}{n_1 kT} \right) - 1 \right] - I_{\mathrm{rs}_2} \left[\exp\left(\frac{(V_L + I_L R_{\mathrm{se}}) \cdot q}{n_2 kT} \right) - 1 \right] - \frac{V_L + I_L R_{\mathrm{se}}}{R_{\mathrm{sh}}} \tag{2.8}$$

where seven unknown parameters I_{pg}, I_{rs_1}, I_{rs_2}, R_{se}, R_{sh}, n_1, and n_2 need to be estimated in the DDM.

2.3. TDM

Similar to the DDM, there is another model named three diode model (TDM). The output current of the TDM is calculated as follows:

$$\begin{aligned} I_L = I_{\mathrm{pg}} - I_{\mathrm{rs}_1} \left[\exp\left(\frac{(V_L + I_L R_{\mathrm{se}}) \cdot q}{n_1 kT} \right) - 1 \right] - I_{\mathrm{rs}_2} \left[\exp\left(\frac{(V_L + I_L R_{\mathrm{se}}) \cdot q}{n_2 kT} \right) - 1 \right] \\ - I_{\mathrm{rs}_3} \left[\exp\left(\frac{(V_L + I_L R_{\mathrm{se}}) \cdot q}{n_3 kT} \right) - 1 \right] - \frac{V_L + I_L R_{\mathrm{se}}}{R_{\mathrm{sh}}} \end{aligned} \tag{2.9}$$

where I_{rs_3}, n_3 represent the third diode saturation current and ideal coefficient, respectively. As could be seen, there are nine unknown parameters to be identified.

2.4. PVM

As shown in Figure 2(c), the single PVM is similar to the SDM. The difference is that there are N_s diodes in series and N_p diodes in parallel in PVM. For the single PVM, the manner of calculating the output current I_L is shown as follows [13, 14]:

$$I = I_{pg}N_p - I_{rs}N_p\left[\exp\left(\frac{(V_LN_p + I_LR_{se}N_s)\cdot q}{nN_sN_pkT}\right) - 1\right] - \frac{V_LN_p + I_LR_{se}N_s}{R_{sh}N_s} \tag{2.10}$$

where there are five unknown parameters like the SDM need to be estimated.

In addition, the double-diode and three-diode based PVM are similar to the DDM and TDM. Note that the N_s and N_p are set to 1 for the single, double, and three diode model, except the PVM.

2.5. Optimization objectives

When employing the heuristic method to estimate the unknown parameters of PV models, the optimization objective need to be developed first. In general, for the PV model optimization, we need to minimize the error between the experimentally measured output current and the output current obtained through simulation. Thus, the error function $f(*)$ of the measured and simulated current data should be defined, which is shown as follows:

- SDM:

$$f(V_L, I_L, \mathbf{x}) = I_{pg} - I_{rs}\left[\exp\left(\frac{(V_L + I_LR_{se})\cdot q}{nkT}\right) - 1\right] - \frac{V_L + I_LR_{se}}{R_{sh}} - I_M \tag{2.11}$$

- DDM:

$$f(V_L, I_L, \mathbf{x}) = I_{pg} - I_{rs_1}\left[\exp\left(\frac{(V_L + I_LR_{se})\cdot q}{n_1kT}\right) - 1\right] - I_{rs_2}\left[\exp\left(\frac{(V_L + I_LR_{se})\cdot q}{n_2kT}\right) - 1\right] - \frac{V_L + I_LR_{se}}{R_{sh}} - I_M \tag{2.12}$$

- TDM:

$$\begin{aligned} f(V_L, I_L, \mathbf{x}) = I_{pg} - I_{rs_1}&\left[\exp\left(\frac{(V_L + I_LR_{se})\cdot q}{n_1kT}\right) - 1\right] - I_{rs_2}\left[\exp\left(\frac{(V_L + I_LR_{se})\cdot q}{n_2kT}\right) - 1\right] \\ &- I_{rs_3}\left[\exp\left(\frac{(V_L + I_LR_{se})\cdot q}{n_3kT}\right) - 1\right] - \frac{V_L + I_LR_{se}}{R_{sh}} - I_M \end{aligned} \tag{2.13}$$

- SPVM:

$$f(V_L, I_L, \mathbf{x}) = I_{pg}N_p - I_{rs}N_p\left[\exp\left(\frac{(V_LN_p + I_LR_{se}N_s)\cdot q}{nN_sN_pkT}\right) - 1\right] - \frac{V_LN_p + I_LR_{se}N_s}{R_{sh}N_s} - I_M \tag{2.14}$$

where $\mathbf{x}$ is a vector containing unknown parameters to be estimated, and I_M is the simulated current which is calculated by substituting the value of unknown parameters estimated by the proposed ERao-1 algorithm into Eqs. (2.4), (2.8), (2.9), and (2.10).

Then, in order to better reflect the overall error between the measured current data and the simulated current data, in this paper, the root mean square error (RMSE) has been employed as the objective function, which has been used in many published literature [26, 27, 9, 28, 29, 30, 30, 4, 31, 14, 16, 19, 32, 17, 15, 33, 18, 20, 34, 35]. The definition of RMSE is shown as follows

$$\text{minimize} \quad \text{RMSE}(\mathbf{x}) = \sqrt{\frac{1}{N}\sum_{i=1}^{N}(f(V_{L_i}, I_{L_i}, \mathbf{x}) - I_{M_i})^2} \tag{2.15}$$

where N represents the number of datasets used in the experiment.

From Eq. (2.15), it can be concluded that the smaller RMSE value the more accurate of the estimated parameters are.

3. Rao-1 algorithm

Rao algorithm as a simple but effective heuristic algorithm was proposed by Rao in 2020 [21]. In the Rao algorithm, there are three sub-algorithms called Rao-1, Rao-2, and Rao-3. Different from Rao-2 and Rao-3, the structure of Rao-1 is simple and has a fast convergence, so the Rao-1 algorithm has attracted much attention. In Rao-1 algorithm, there are three core operations including population initialization, evolution operator, and selection, which are briefly introduced in the following section.

3.1. Population initialization

Assume that there are np individuals in a population $\mathbb{P}$, where each individual can be seen as a D-dimension vector. In this regard, noting that each individual can be considered a candidate solution. In population initialization, each individual is initialized in a given search space. For example, the i-th individual is initialized as follows

$$x_{i,j} = a_j + r \cdot (b_j - a_j), \ \ j \in [1, D] \tag{3.1}$$

where a_j and b_j represent the low bound and upper bound of the j-dimension, respectively. While r is a random number between 0 and 1.

3.2. Evolution operator

Evolution operator is a core operator in Rao-1 algorithm, which is used to generate the promising offspring. The idea of this operator comes from the learning experience that the worst individual in the population learns from the best individual. For example, the i-th individual's evolution operator is formulated as follows

$$x'_{i,j} = x_{i,j} + r_j \cdot (x_{\text{best},j} - x_{\text{worst},j}) \tag{3.2}$$

where $\mathbf{x}'_i$ denotes the i-th individual after evolution operator, r_j is a random number between 0 and 1 in the j-dimension, $\mathbf{x}_{\text{best}}$ and $\mathbf{x}_{\text{worst}}$ are the best and worst individual in the population $\mathbb{P}$, which is done according to the objective function value in ascending order.

Then, the generated $\mathbf{x}_i'$ may will be checked for outside the specific search space. If $\mathbf{x}_i'$ oversteps the search bounds at the j-dimension, then the j-dimension of $\mathbf{x}_i'$ will be re-initialized using Eq. (3.1).

3.3. Selection

After the evolution operator, all newly generated $\mathbf{x}_i'$ are evaluated by calculating the fitness value (objective function value in this paper). Thereafter, the algorithm will decide whether the original individual $\mathbf{x}_i$ or the new individual $\mathbf{x}_i'$ survives the next generation. In Rao-1 algorithm, the one to one greedy choice strategy is adopted, which is expressed as follows:

$$\mathbf{x}_i = \begin{cases} \mathbf{x}_i', & \text{if } f(\mathbf{x}_i') \leq f(\mathbf{x}_i) \\ \mathbf{x}_i, & \text{otherwise} \end{cases} \tag{3.3}$$

where the $\mathbf{x}_i$ after selection operator will be used as the individual in the next generation population.

4. Enhanced Rao-1 algorithm

4.1. Motivations

Despite the success enjoyed by Rao-1 algorithm, it is worth noting that there are three points worth further studying. Firstly, the evolution operator in Rao-1 algorithm has too much randomness. From Eq. (3.2), it can be seen that each dimension of the new generated individual is produced by the dimension of best and worst individuals with a random number. If the dimension of the problem is higher, the greater the randomness of each dimension. Due to randomness improvements in other dimensions, improvements in one dimension may result in poor performance. Secondly, in Rao-1 algorithm, there is only one evolution operator shown as Eq. (3.2), namely only use the best and worst individuals to guide searching, which may result in the algorithm not being able to balance exploration and exploitation capabilities well. Thirdly, although the Rao-1 algorithm enjoyed the parameter-free when compared many heuristic methods, there is still a common parameter namely population size np that needs to be set by user. Taking above points into consideration, an enhanced Rao-1 algorithm referred as ERao-1 is proposed. In ERao-1, a repaired evolution operator is presented to reduce the randomness in Rao-1 algorithm. Then a new evolution operator is developed to prevent the Rao-1 algorithm from falling into local optimum. Finally, the population size linear reduction strategy is employed to adaptively adjust the population size as it evolves. A detailed description about these improvements will be introduced in following sections.

4.2. Repaired evolution operator

To reduce the randomness of Rao-1 algorithm, in this subsection, a repaired evolution operator is presented. In the repaired evolution operator, there is only a random number r on all dimensions rather than j random numbers on each dimension. The repaired evolution operator is formulated as follows

$$\mathbf{x}_i' = \mathbf{x}_i + r \cdot (\mathbf{x}_{\text{best}} - \mathbf{x}_{\text{worst}}) \tag{4.1}$$

where r is a random number in interval 0 to 1.

From Eq. (4.1), it is straightforward to see that the new individual $\mathbf{x}_i'$ is generated by a random number r through the differential vector of the $\mathbf{x}_{\text{best}}$ and $\mathbf{x}_{\text{worst}}$. In this way, a large amount of randomness in the Rao-1 algorithm can be avoided, thus speeding up the convergence of the algorithm.

4.3. New evolution operator

As mentioned earlier, there is only a single evolution operator in the Rao-1 algorithm, which may not be a good compromise between the exploitation and the exploration. In addition, in Eq. (3.2), only the best and the worst individuals are used to guide search, which may lead to under-utilization of information from other individuals in the population and easy to trap into local optimum. Inspired by the mutation in DE [36, 37], a new evolution operator is proposed, which is defined as below

$$\mathbf{x}_i' = \mathbf{x}_i + r_1 \cdot (\mathbf{x}_{\text{best}} - \mathbf{x}_{\text{worst}}) + r_2 \cdot (\mathbf{x}_p - \mathbf{x}_q) \tag{4.2}$$

where r_1 and r_2 are two random numbers between 0 and 1. $\mathbf{x}_p$ and $\mathbf{x}_q$ are two individuals randomly selected from the current population $\mathbb{P}$, and $f(\mathbf{x}_p) \leq f(\mathbf{x}_q)$. Noting that $p \neq q \neq i$.

From Eq. (4.2), it can be seen that there is another differential vector $(\mathbf{x}_p - \mathbf{x}_q)$ that is used to guide search. There are two benefits that can be obtained from the new evolution operator. On the one hand, it can make better use of the information of other individuals in the population. On the other hand, it can avoid the algorithm falling into local optimum. However, it should be pointed out that this new evolution operator may slow down the convergence speed. Thus, to alleviate the situation, the repaired evolution operator and the new evolution operator are called adaptively according to the individuals objective function values, which is shown as

$$\mathbf{x}_i = \begin{cases} \mathbf{x}_i + r_1 \cdot (\mathbf{x}_{\text{best}} - \mathbf{x}_{\text{worst}}) + r_2 \cdot (\mathbf{x}_p - \mathbf{x}_q), & \text{if } ind(i) < np/2 \\ \mathbf{x}_i + r \cdot (\mathbf{x}_{\text{best}} - \mathbf{x}_{\text{worst}}), & \text{otherwise} \end{cases} \tag{4.3}$$

where $ind(i)$ represents the index of the i-th individual objective function value sorted in ascending order.

From Eq. (4.3), it is clear that the better individuals adopt the new evolution operator to prevent from falling into local optimum while the worse individuals take the repaired evolution operator to accelerate convergence. By this way, the exploitation and exploration abilities can be made a good tradeoff.

4.4. Population size linear reduction strategy

In order to make the Rao-1 algorithm parameter-free, in this subsection, a population size linear reduction strategy is employed. In this strategy, the population size np decreases linearly with evolution process. Given that the current population size is np_G, np_{G+1} is the next generation population size, which is updated as Eq. (4.4)

$$np_{G+1} = round\left[np_{\max} - \left(\frac{np_{max} - np_{\min}}{M\_FEs}\right) \cdot FEs\right] \tag{4.4}$$

where $np_{\max}$ and $np_{\min}$ denote the the maximum population size and the minimum population size, respectively. While FEs and M_FEs represent the number of function evaluations currently called and the allow maximum number of function evaluations, respectively.

4.5. Overview of proposed ERao-1 algorithm

The main three improvements have been described in above section, then based on these improvements, the enhanced Rao-1 algorithm namely ERao-1 is proposed. **Algorithm 1** provides the pseudo-code of the proposed ERao-1 algorithm, where it can be observed that the proposed ERao-1 algorithm does not introduce new parameters, and it still has a simple structure. Noting that the repaired evolution operator and new evolution operator are used in lines 9-12, while the population size linear reduction strategy is used in line 17. In addition, as for the algorithm complexity, the Rao-1 algorithm complexity is $O(G_{max} \cdot np \cdot D)$, where G_{max} is the maximum number of generations and it can be calculated as $G_{max} = M\_FEs/np$. Since the proposed ERao-1 algorithm does not introduce other additional computational burdens. Therefore, the algorithm complexity of ERao-1 is also $O(G_{max} \cdot np \cdot D)$.

Algorithm 1: The pseudo-code of ERao-1 algorithm

Input: Control parameters: M_FEs

Output: Optimal estimated parameters

1 load the measured $V_L - I_L$ data;
2 Set $FEs = 0, np = np_{\max} = 30, np_{min} = 3$;
3 Randomly initialize the population $\mathbb{P}$ using Eq. (3.1);
4 Using Eq. (2.15) to evaluate each individual in $\mathbb{P}$;
5 $FEs = FEs + np$;
6 **while** $FEs < M\_FEs$ **do**
7 **for** $i = 1$ *to* np **do**
8 Sort the population $\mathbb{P}$ according to the objective function values to get the index ind;
9 **if** $ind(i) < np/2$ **then**
10 Using the new evolution operator Eq. (4.2) to generate $\mathbf{x}_i'$;
11 **else**
12 Using the repaired evolution operator Eq. (4.1) to generate $\mathbf{x}_i'$;
13 Using Eq. (3.1) to deal with the generated $\mathbf{x}_i'$;
14 Evaluate the generated $\mathbf{x}_i'$ using Eq. (2.15);
15 Selection using Eq. (3.3);
16 $FEs = FEs + np$;
17 Update the population size np using Eq. (4.4);

5. Experiments and results

With the aim of verifying the performance of proposed ERao-1 algorithm, it is evaluated by estimating the unknown parameters of three different PV models including SDM, DDM, TDM, and its expansion in PVM. First, the 57 mm diameter commercial R.T.C France silicon cell is selected, where there are 26 pairs of V_L-I_L data that are measured under 1000 W/m^2 at 33 °C. For the PVM, the polycrystalline Photowatt-PWP201 is selected, where there are 25 pairs of V_L-I_L data that are measured under 1000 W/m^2 at 45 °C. In addition, the search ranges of unknown parameters are given in Table 1.

As for the comparison algorithms, in this paper, seven well-established parameter estimation meth-

Table 1. Search ranges of unknown parameters.

Parameter	R.T.C France silicon cell		Photowatt-PWP201 cell	
	a	*b*	*a*	*b*
I_{pg} (A)	0	1	0	2
I_{rs}, I_{rs1}, I_{rs2}, I_{rs3} (μA)	0	1	0	50
R_{se} (Ω)	0	0.5	0	2
R_{sh} (Ω)	0	100	0	2000
n, n_1, n_2, n_3	1	2	1	50

ods including GOTLBO [15], IJAYA [16], MLBSA [17], TLABC [18], PGJAYA [19], ITLBO [20], and original Rao-1 algorithm [21] are selected. Table 2 gives the experimental settings of these algorithms. Note that these settings are kept consistent with their corresponding literatures. In addition, for fair comparison, all comparison algorithms are implemented by using MATLAB2016 software, and the allow maximum M_FEs is set to be 30,000 for all PV models. It is worth mentioning that all experiment are conducted on a desktop PC with an Intel Core i7-9700M processor @ 3.0 GHz, 32GB RAM, under the Windows 10 64-bit operating system.

Table 2. Experimental settings of comparison algorithms.

Algorithm	Settings
GOTLBO	np = 50, jumping rate Jr = 0.3
IJAYA	np = 20
MLBSA	np = 50
TLABC	np =50, limit=200, scale factor F = rand(0,1)
PGJAYA	np = 20
ITLBO	np = 50
Rao-1	np = 30
ERao-1	np_{max} = 30, np_{min} = 3

5.1. Results on the R.T.C France silicon cell

5.1.1. Results on the SDM of the R.T.C France silicon cell

As mentioned beforehand, five unknown parameters need to be estimated in the SDM. Table 3 reports the comparison results of ERao-1 and its competitors, where the best objective function value (RMSE) and corresponding estimated parameter values are involved. Noting that the best RMSE value has been marked in black bold. From Table 3, it can be observed that ERao-1, ITLBO, PGJAYA, TLABC, MLBSA, and GOTLBO are able to obtain the same best RMSE value (9.8602E-04), followed by IJAYA (9.8626E-04), and Rao-1 (1.1478E-03). Although the difference of IJAYA and ERao-1 is particularly small i.e., 2.4E-07, it still makes sense. As mentioned in subsection 2.5, the smaller RMSE value the more accurate the estimated parameters are. Besides, since the true parameter value is not available, any reduction in the objective function value means that the estimated parameter value is

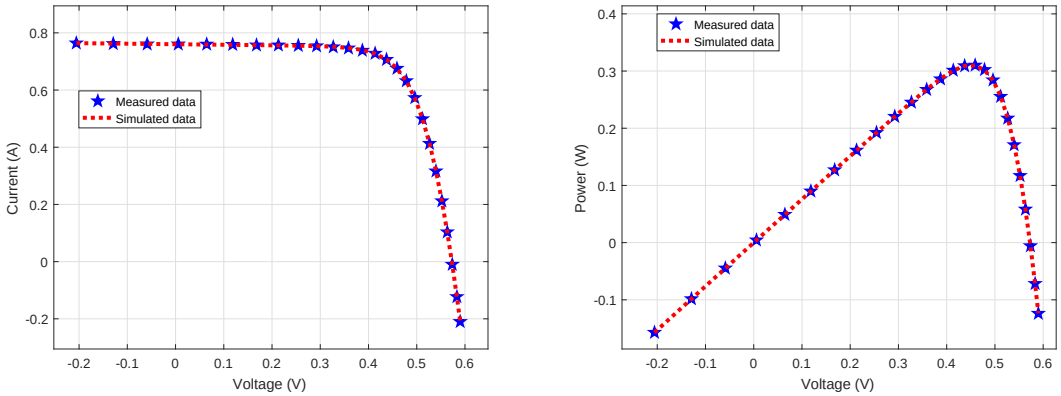

(a) Fitting curve of voltage-current (b) Fitting curve of voltage-power

Figure 3. The fitting curves of the measured data and simulated data on the SDM of the R.T.C France silicon cell.

more accurate. In addition, when compared with the original Rao-1 algorithm, it is clear that the enhanced Rao-1 algorithm has significant performance improvement.

Table 3. Estimated parameters achieved by ERao-1 and compared algorithms on the SDM of the R.T.C France silicon cell.

Algorithm	I_{pg} (A)	I_{rs} (μA)	R_{se} (Ω)	R_{sh} (Ω)	n	RMSE
GOTLBO	0.7608	0.3230	0.0364	53.7185	1.4812	**9.8602E-04**
IJAYA	0.7608	0.3240	0.0364	53.6555	1.4815	9.8626E-04
MLBSA	0.7608	0.3230	0.0364	53.7185	1.4812	**9.8602E-04**
TLABC	0.7608	0.3230	0.0364	53.7185	1.4812	**9.8602E-04**
PGJAYA	0.7608	0.3230	0.0364	53.7186	1.4812	**9.8602E-04**
ITLBO	0.7608	0.3230	0.0364	53.7185	1.4812	**9.8602E-04**
Rao-1	0.7607	0.4176	0.0353	64.9212	1.5075	1.1478E-03
ERao-1	0.7608	0.3230	0.0364	53.7185	1.4812	**9.8602E-04**

To further explain the accuracy of the estimated parameters of ERao-1 algorithm, we calculate the simulated current data by using the parameters estimated by the ERao-1 algorithm to substitute into Eq. (2.4). Then, draw the fitting curve between the simulation data and the measured data shown as Figure 3. From Figure 3(a), it can be seen that the simulated current data provided by ERao-1 is able to fit the measured current data well. Also, the simulated power data and the measured power data have a good consistency, which can be observed from Figure 3(b). Based on the above findings, it can conclude that the estimated parameters by ERao-1 are very accurate for the SDM.

5.1.2. Results on the DDM of the R.T.C France silicon cell

For the DDM, seven unknown parameters I_{pg}, I_{rs_1}, I_{rs_2}, R_{se}, R_{sh}, n_1, and n_2 must be estimated. Obviously, compared with the SDM, the DDM has two additional unknown parameters including I_{rs_2} and n_2

need to be estimated, which means that the dimension of the problem has increased. It is noteworthy that the increase in dimensions can lead to the complexity of the problem. Table 4 provides the estimated parameters achieved by ERao-1 and other compared algorithms. From this table, it is evident that only ERao-1 algorithm can achieve the best RMSE value (9.8248E-04) on this model, followed by ITLBO (9.8250E-04), PGJAYA (9.8286E-04), TLABC (9.8317E-04), GOTLBO (9.8401E-04), IJAYA (9.8655E-04), and Rao-1 (1.2087E-03). According to this findings, it can be seen that the performance of most well-established parameter estimation algorithms is affected by the increase of problem dimensions while the proposed algorithm still has good performance. Moreover, it is remarkable that the performance of ERao-1 is also significantly superior to the original Rao-1 algorithm on the DDM.

Table 4. Estimated parameters achieved by ERao-1 and compared algorithms on the DDM of the R.T.C France silicon cell.

Algorithm	I_{pg} (A)	I_{rs1} (μA)	R_{se}	R_{sh} (Ω)	n_1	I_{rs2} (μA)	n_2	RMSE
GOTLBO	0.7608	0.2470	0.0366	54.6570	1.4595	0.3443	1.8749	9.8401E-04
IJAYA	0.7607	0.0002	0.0363	53.8328	1.4817	0.3247	1.7891	9.8655E-04
MLBSA	0.7608	0.2863	0.0365	54.3445	1.4710	0.2756	1.9991	9.8424E-04
TLABC	0.7608	0.6052	0.0367	55.2625	1.4506	0.2235	1.9401	9.8317E-04
PGJAYA	0.7608	0.2531	0.0366	55.1223	1.4606	0.5341	2.0000	9.8286E-04
ITLBO	0.7608	0.2316	0.0367	55.3661	1.4531	0.7021	2.0000	9.8250E-04
Rao-1	0.7613	0.2799	0.0355	55.3796	1.4968	0.3686	1.9766	1.2087E-03
ERao-1	0.7608	0.2260	0.0367	55.4854	1.4510	0.7493	2.0000	**9.8248E-04**

In addition, similar to the SDM, the simulated current data is calculated by using the parameters estimated by the ERao-1 algorithm to substitute into Eq. (2.8) for the DDM. Figure 4 plots the fitting curve between the simulated data and the measured data. From this figure, it is evident that the simulated data are highly consistent with the measured data, both for the current data and the power data. Therefor, it can be concluded that the estimated parameters obtained by ERao-1 are pretty accurate for the DDM.

5.1.3. Results on the TDM of the R.T.C France silicon cell

Table 5 reports the results on the TDM of the R.T.C France silicon cell, where it can observe that ERao-1 achieves the best performance (9.8257E-04) on this model, followed by ITLBO (9.8260E-04), MLBSA (9.8286E-04), PGJAYA (9.8351E-04), IJAYA (9.8451E-04), GOTLBO (9.8562E-04), and TLABC (9.8622E-04). Note that although the dimension in the TDM is increased to nine dimensions, the proposed algorithm can still provide the smallest RMSE value. Besides, from the Figure 5, it is clear that the simulated data obtained by ERao-1 is also consistent with the measured data.

5.2. Results on the Photowatt-PWP201 cell

5.2.1. Results on the single PVM of the Photowatt-PWP201

The comparison results of ERao-1, GOTLBO, IJAYA, MLBSA, TLABC, PGJAYA, ITLBO, and Rao-1 are reported in Table 6, where what can be observed is that all algorithms can provide the best RMSE value (2.4251E-03) except the IJAYA (2.4254E-03) and Rao-1 (2.4418E-03). It can be

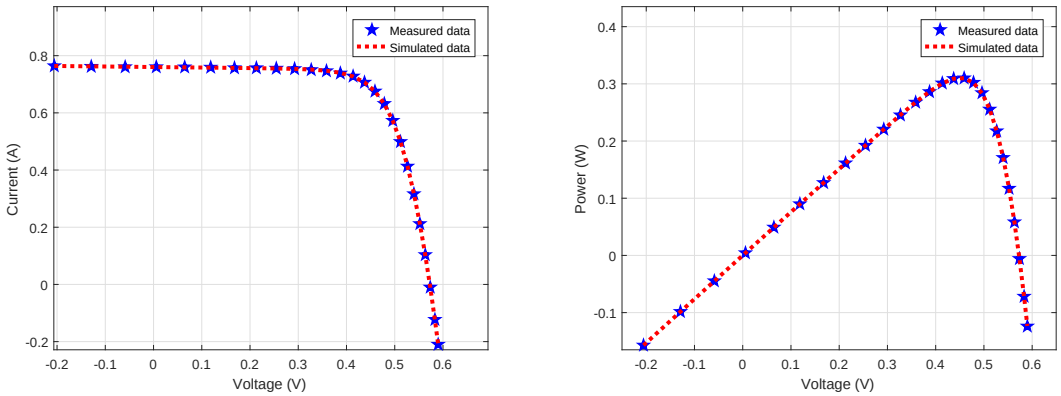

(a) Fitting curve of voltage-current (b) Fitting curve of voltage-power

Figure 4. The fitting curves of the measured data and simulated data on the DDM of the R.T.C France silicon cell.

Table 5. Estimated parameters achieved by ERao-1 and compared algorithms on the TDM of the R.T.C France silicon cell.

Algorithm	I_{pg} (A)	I_{rs1} (μA)	R_{se}	R_{sh} (Ω)	n_1	I_{rs2} (μA)	n_2	I_{rs3} (μA)	n_3	RMSE
GOTLBO	0.7608	0.1804	0.0366	54.5868	1.4411	0.1870	1.6582	0.1122	1.7383	9.8562E-04
IJAYA	0.7607	0.1739	0.0366	55.0750	1.8796	0.2484	1.4594	0.2703	1.9995	9.8451E-04
MLBSA	0.7608	0.9452	0.0369	56.1208	1.9987	0.2020	1.4417	0.0107	1.9996	9.8286E-04
TLABC	0.7608	0.2898	0.0367	55.8789	1.7438	0.1824	1.8668	0.1834	1.4388	9.8622E-04
PGJAYA	0.7608	0.0024	0.0365	54.6491	1.9341	0.2740	1.4672	0.0364	2.0000	9.8351E-04
ITLBO	0.7608	0.4404	0.0367	55.3099	2.0000	0.2354	1.9956	0.2342	1.4540	9.8260E-04
Rao-1	0.7603	0.1833	0.0367	65.3903	1.8100	0.1509	1.4517	0.1576	1.5204	1.4205E-03
ERao-1	0.7608	0.2092	0.0368	55.6504	1.4466	0.0108	1.5108	0.8108	2.0000	**9.8257E-04**

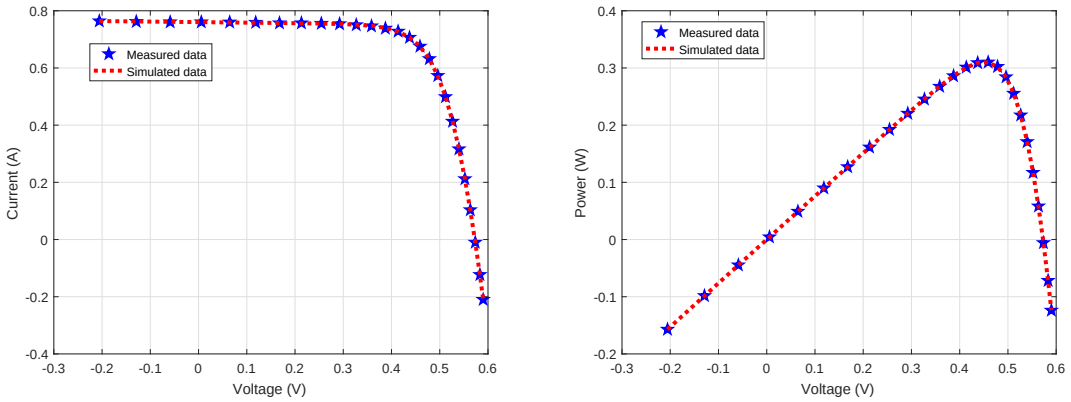

(a) Fitting curve of voltage-current (b) Fitting curve of voltage-power

Figure 5. The fitting curves of the measured data and simulated data on the TDM of the R.T.C France silicon cell.

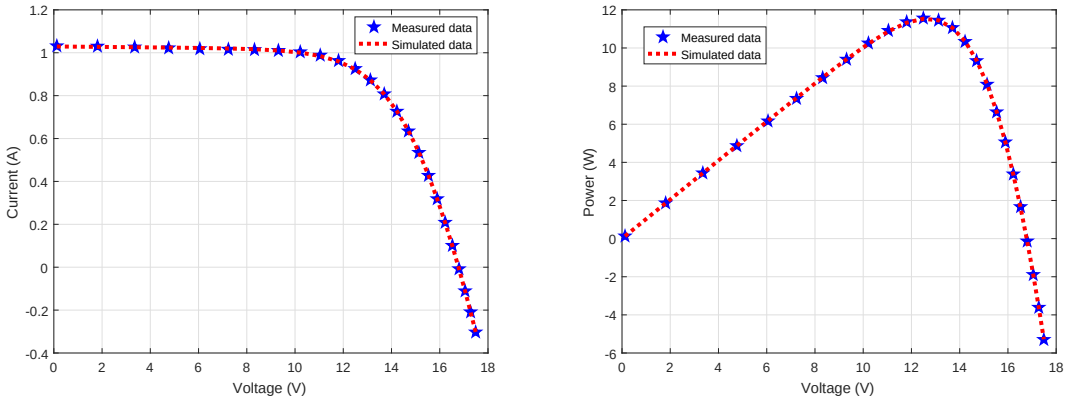

(a) Fitting curve of voltage-current (b) Fitting curve of voltage-power

Figure 6. The fitting curves of the measured data and simulated data on the SPVM.

concluded that the enhanced ERao-1 algorithm performs better than IJAYA, and comparable to other algorithms such as GOTLBO, MLBSA, TLABC, PGJAYA, and ITLBO for the single PVM. In addition, Figure 6 draws the fitting curve between the simulated current (power) data and the measured current (power) data. From Figure 6, it can be seen that the simulated current (power) data provided by ERao-1 is well agreed with the current (power) data, which also demonstrates that ERao-1 can provide pretty accurate parameter values for the single PVM.

Table 6. Estimated parameters achieved by ERao-1 and compared algorithms on the single PVM of the Photowatt-PWP201 cell.

Algorithm	I_{pg} (A)	I_{rs} (μA)	R_{se} (Ω)	R_{sh} (Ω)	n	RMSE
GOTLBO	1.0305	3.4823	1.2013	981.9823	48.6428	**2.4251E-03**
IJAYA	1.0306	3.4594	1.2021	970.0370	48.6176	2.4254E-03
MLBSA	1.0305	3.4823	1.2013	981.9820	48.6428	**2.4251E-03**
TLABC	1.0305	3.4823	1.2013	981.9823	48.6428	**2.4251E-03**
PGJAYA	1.0305	3.4817	1.2013	981.7622	48.6422	**2.4251E-03**
ITLBO	1.0305	3.4823	1.2013	981.9822	48.6428	**2.4251E-03**
Rao-1	1.0300	3.5278	1.1994	1024.4284	48.6910	2.4418E-03
ERao-1	1.0305	3.4823	1.2013	981.9822	48.6428	**2.4251E-03**

5.2.2. Results on the double PVM of the Photowatt-PWP201

The results on the double PVM of the Photowatt-PWP201 are provided in Table 7. From this table, GOTLBO, PGJAYA, ITLBO, and proposed ERao-1 algorithms can provide the smallest RMSE value (2.4251E-03). MLBSA and TLABC achieved the best results in the single PVM while it does not achieve the best performance on this model. In addition, it is worth mentioning that the optimal value of the double PVM of the Photowatt-PWP201 is almost the single PVM. Lastly, from the fitting curves of ERao-1 shown in Figure 7, it also fits the measured data very well, both for voltage-current and

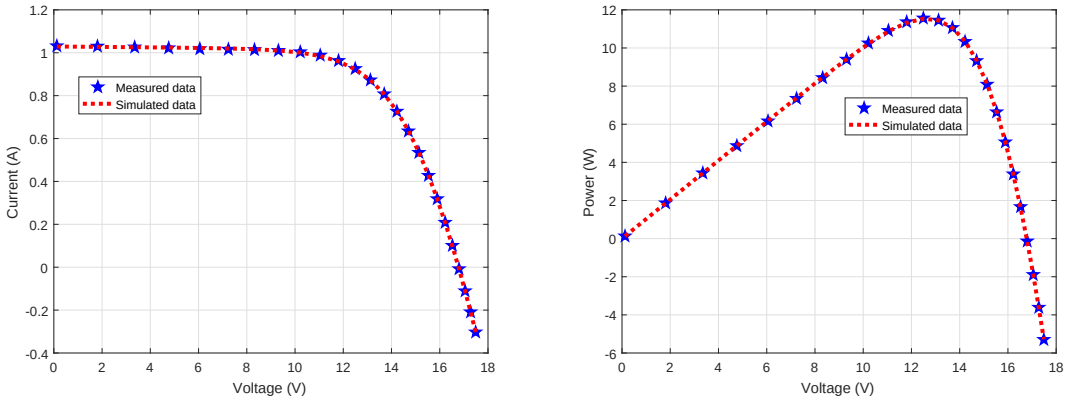

(a) Fitting curve of voltage-current (b) Fitting curve of voltage-power

Figure 7. The fitting curves of the measured data and simulated data on the double PVM of the Photowatt-PWP201 cell.

voltage-power.

Table 7. Estimated parameters achieved by ERao-1 and compared algorithms on the double PVM of the Photowatt-PWP201 cell.

Algorithm	I_{pg} (A)	I_{rs1} (μA)	R_{se}	R_{sh} (Ω)	n_1	I_{rs2} (μA)	n_2	RMSE
GOTLBO	1.0305	2.1004	1.2013	982.0163	48.6514	1.3824	48.6313	**2.4251E-03**
IJAYA	1.0303	0.0258	1.2005	1017.3298	49.9869	3.5002	48.6823	2.4265E-03
MLBSA	1.0306	0.0000	1.2021	974.3427	18.1787	3.4565	48.6144	2.4254E-03
TLABC	1.0306	3.4405	1.2025	967.8519	48.5968	0.1100	43.0812	2.4253E-03
PGJAYA	1.0305	0.6276	1.2015	976.6385	48.4807	2.8456	48.6676	**2.4251E-03**
ITLBO	1.0305	2.6303	1.2013	981.9822	48.6428	0.8519	48.6428	**2.4251E-03**
Rao-1	1.0286	0.5738	1.1878	1398.3744	48.7330	3.5520	49.3947	2.5075E-03
ERao-1	1.0305	3.2619	1.2013	981.9822	48.6428	0.2203	48.6428	**2.4251E-03**

5.2.3. Results on the three PVM of the Photowatt-PWP201

For the three PVM of the Photowatt-PWP201, there are also nine unknown parameters including the I_{pg}, I_{rs_1}, I_{rs_2}, I_{rs_3}, R_{se}, R_{sh}, n_1, n_2, and n_3 that need to be estimated. The comparison results of proposed ERao-1 and other state-of-the-art algorithms are given in Table 8, where it is obvious that only MLBSA and ERao-1 are able to achieve the best RMSE value (2.4251E-03), followed by ITLBO (2.4252E-03), PGJAYA (2.4253E-03), IJAYA (2.4254E-03), GOTLBO (2.4257E-03), TLABC (2.4329E-03), and Rao-1 (2.4905E-03). In particular, when comparing with the original Rao-1 algorithm, the proposed ERao-1 has a significant performance superiority. Further, the fitting curves of ERao-1 plotted in Figure 8 also prove the accuracy of its identified parameters.

Table 8. Estimated parameters achieved by ERao-1 and compared algorithms on the three PVM of the Photowatt-PWP201 cell.

Algorithm	I_{pg} (A)	I_{rs1} (μA)	R_{se}	R_{sh} (Ω)	n_1	I_{rs2} (μA)	n_2	I_{rs3} (μA)	n_3	RMSE
GOTLBO	1.0307	0.0001	1.2025	956.9990	48.3808	0.3869	49.0381	3.0482	48.5387	2.4257E-03
IJAYA	1.0305	1.1725	1.2009	986.4440	48.9538	2.3266	48.5232	0.0000	1.0000	2.4254E-03
MLBSA	1.0305	0.0000	1.2013	982.0953	49.8462	3.4824	48.6430	0.0000	9.6969	**2.4251E-03**
TLABC	1.0305	2.7339	1.2016	993.5425	49.2577	0.3163	46.1710	0.5671	48.9363	2.4329E-03
PGJAYA	1.0305	0.0000	1.2002	991.8341	45.2952	3.5117	48.6863	0.0077	47.6045	2.4253E-03
ITLBO	1.0305	0.0004	1.2018	978.6182	43.4304	3.4684	48.6295	0.0000	46.6646	2.4252E-03
Rao-1	1.0309	0.1818	1.1946	928.9720	47.3377	1.3244	48.1476	2.2048	49.6399	2.4905E-03
ERao-1	1.0305	0.0000	1.2013	981.9823	48.8882	1.5794	48.6428	1.9029	48.6428	**2.4251E-03**

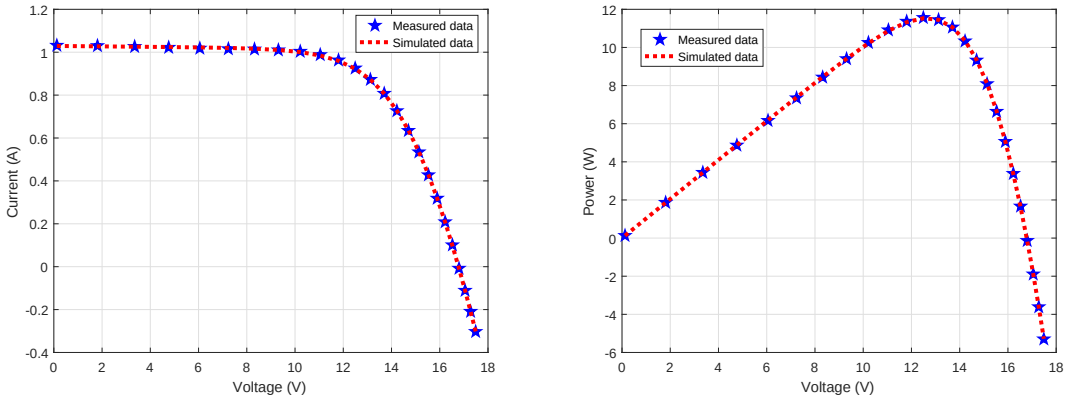

(a) Fitting curve of voltage-current

(b) Fitting curve of voltage-power

Figure 8. The fitting curves of the measured data and simulated data on the three PVM of the Photowatt-PWP201 cell.

5.3. Statistical results analysis

From subsection 5.1-5.2, we have analyzed the best RMSE value of ERao-1 and other well-established approaches. Based on above analysis, we can find that some algorithms such as GOTLBO, MLBSA, TLABC, PGJAYA, and ITLBO can achieve the best result like ERao-1, especially for the SDM and single PVM. In the context of this, in order to further show the superiority of the proposed ERao-1 algorithm, the statistical results analysis such as the minimum RMSE (Min), maximum RMSE (Max), average RMSE (Ave), standard deviation (Std), FEs to reach the optimal solution (FEs), CPU time of 30 times independent runs, and two non-parametric statistical tests namely Wilcoxon signed-ranks test and Friedman Aligned test are conducted. Noting that all algorithm are run independently 30 times under the above mentioned experimental environment, and the non-parametric statistical test is carried out by the KEEL tool [38]. In addition, the convergence curves of all compared algorithms on different PV models are plotted.

Table 9. Statistical results achieved by ERao-1 and compared algorithms on the R.T.C France silicon cell.

Model	Algorithm	RMSE				FEs	CPU time (s)	Wilcoxon Signed Ranks test			
		Min	Max	Mean	Std			R^+	R^-	p-value	Sig.
SDM	GOTLBO	**9.86021878E-04**	1.13918657E-03	1.00159113E-03	3.34E-05	28906	2.07	397.0	68.0	3.80E-04	+
	IJAYA	9.86257498E-04	1.16541327E-03	1.01536934E-03	3.96E-05	30000	4.31	465.0	0.0	1.86E-09	+
	MLBSA	**9.86021878E-04**	9.98586264E-04	9.86927884E-04	2.47E-06	30000	6.67	426.0	39.0	1.40E-05	+
	TLABC	**9.86021878E-04**	1.36553943E-03	1.04841480E-03	9.79E-05	30000	13.41	454.5	10.5	9.13E-08	+
	PGJAYA	**9.86021878E-04**	9.89166838E-04	9.86309825E-04	6.68E-07	30000	2.49	430.0	5.0	3.73E-08	+
	ITLBO	**9.86021878E-04**	**9.86021878E-04**	**9.86021878E-04**	2.57E-17	20452	2.92	232.5	232.5	≥ 0.2	$\approx$
	Rao-1	1.14778123E-03	2.10098078E-03	1.37929726E-03	2.00E-04	30000	1.54	465.0	0.0	1.86E-09	+
	ERao-1	**9.86021878E-04**	**9.86021878E-04**	**9.86021878E-04**	**2.13E-17**	6735	5.76				
DDM	GOTLBO	9.84007532E-04	2.02180375E-03	1.21589875E-03	3.03E-04	30000	2.37	447.0	18.0	4.71E-07	+
	IJAYA	9.86551948E-04	1.38705516E-03	1.09860914E-03	1.31E-04	30000	4.94	465.0	0.0	1.86E-09	+
	MLBSA	9.84240741E-04	1.37423619E-03	1.00561219E-03	7.25E-05	30000	7.70	396.0	69.0	4.18E-04	+
	TLABC	9.83167498E-04	2.71422115E-03	1.19318928E-03	3.83E-04	30000	13.64	443.0	22.0	9.98E-07	+
	PGJAYA	9.82864797E-04	1.04716705E-03	9.89906250E-04	1.18E-05	30000	2.78	401.0	64.0	2.56E-04	+
	ITLBO	9.82504296E-04	1.00042927E-03	9.85663194E-04	3.08E-06	30000	3.15	259.0	176.0	≥ 0.2	$\approx$
	Rao-1	1.20872604E-03	2.76432400E-03	1.75883822E-03	3.79E-04	30000	1.83	465.0	0.0	1.86E-09	+
	ERao-1	**9.82484852E-04**	**9.89138102E-04**	**9.84975061E-04**	**1.75E-06**	30000	5.84				
TDM	GOTLBO	9.85618492E-04	3.73585977E-03	1.60977967E-03	7.81E-04	30000	2.66	412.0	23.0	2.38E-06	+
	IJAYA	9.84513706E-04	1.48969353E-03	1.15827319E-03	1.57E-04	30000	5.29	462.0	3.0	9.31E-09	+
	MLBSA	9.82863342E-04	1.25317389E-03	1.00444139E-03	5.20E-05	30000	8.18	333.0	132.0	3.84E-02	+
	TLABC	9.86215434E-04	3.73696660E-03	1.47370620E-03	6.54E-04	30000	14.41	459.0	6.0	2.61E-08	+
	PGJAYA	9.83509044E-04	1.08885492E-03	9.93412110E-04	2.15E-05	30000	3.12	306.0	159.0	1.35E-01	+
	ITLBO	9.82597856E-04	1.30506970E-03	1.01123804E-03	7.37E-05	30000	3.60	257.0	208.0	≥ 0.2	$\approx$
	Rao-1	1.42051514E-03	3.22942508E-03	2.30993781E-03	4.77E-04	30000	2.20	465.0	0.0	1.86E-09	+
	ERao-1	**9.82572360E-04**	**1.02338992E-03**	**9.87592443E-04**	**7.64E-06**	30000	6.11				

Table 9 and Table 10 report the statistical results, where the Min, Max, Ave, Std, FEs, CPU time, and Wilcoxon signed-ranks test results are provided, where R^+ (R^-) is the sum of ranks for the optimization objective on which ERao-1 outperforms (loses) its competitors, p-value denotes the significance which will decide whether the statistical hypothesis ($\alpha = 5\%$) should be rejected, and "+" and "$\approx$" indicate that ERao-1 significantly performs better or similar to its competitors. From these tables, it can be seen that

- As can be seen from Table 9, for the SDM in R.T.C France silicon cell, it is obvious that most algorithms can get the best Min except IJAYA and Rao-1, while only ERao-1 and ITLBO are capable of achieving the best Max and Ave, especially for Ave that can reflect the accuracy of the algorithm. In addition, from the perspective of the Std, it is clear that ERao-1 and ITLBO have obvious advantages over other algorithms, which indicates that the proposed ERao-1 and

Table 10. Statistical results achieved by ERao-1 and compared algorithms on the Photowatt-PWP201 cell.

Model	Algorithm	RMSE				FEs	CPU time (s)	Wilcoxon Signed Ranks test			
		Min	Max	Mean	Std			R^+	R^-	p-value	Sig.
SDM	GOTLBO	**2.42507487E-03**	3.07572577E-03	2.45462947E-03	1.21E-04	12788	2.05	330.0	105.0	1.38E-02	+
	IJAYA	2.42541187E-03	2.69195878E-03	2.45694390E-03	4.88E-05	30000	4.57	465.0	0.0	1.86E-09	+
	MLBSA	**2.42507487E-03**	9.05516699E-03	2.66367904E-03	1.21E-03	17633	6.68	360.0	105.0	7.61E-03	+
	TLABC	**2.42507487E-03**	2.84110334E-03	2.44752164E-03	7.73E-05	15564	13.32	396.0	39.0	2.78E-05	+
	PGJAYA	2.42507492E-03	2.43377624E-03	2.42596008E-03	1.85E-06	24517	2.49	433.5	1.5	9.31E-09	+
	ITLBO	**2.42507487E-03**	**2.42507487E-03**	**2.42507487E-03**	**1.04E-17**	11166	2.89	232.5	232.5	≥ 0.2	≈
	Rao-1	2.44184971E-03	2.77946734E-03	2.57063490E-03	9.05E-05	30000	1.56	465.0	0.0	1.86E-09	+
	ERao-1	**2.42507487E-03**	**2.42507487E-03**	**2.42507487E-03**	**1.72E-17**	4432	5.77				
DDM	GOTLBO	2.42507552E-03	2.18457789E-02	3.61434948E-03	4.10E-03	24320	2.28	455.0	10.0	8.01E-08	+
	IJAYA	2.42651786E-03	2.86150253E-03	2.48310492E-03	8.42E-05	30000	5.00	465.0	0.0	1.86E-09	+
	MLBSA	2.48921545E-03	8.39623324E-03	2.83716901E-03	1.39E-03	30000	7.59	426.5	38.5	1.31E-05	+
	TLABC	2.42530765E-03	3.65688874E-03	2.65397183E-03	3.74E-04	30000	14.11	452.0	13.0	1.64E-07	+
	PGJAYA	2.42513255E-03	2.46134760E-03	2.43247931E-03	8.70E-06	30000	2.72	465.0	0.0	1.86E-09	+
	ITLBO	**2.42507487E-03**	2.43565714E-03	2.42573456E-03	2.11E-06	16320	3.18	307.0	158.0	1.29E-01	+
	Rao-1	2.50750455E-03	3.05475485E-03	2.67852422E-03	1.54E-04	30000	1.81	465.0	0.0	1.86E-09	+
	ERao-1	**2.42507487E-03**	**2.43551343E-03**	**2.42542540E-03**	**1.91E-06**	10916	5.93				
TDM	GOTLBO	2.42569790E-03	6.91482937E-02	7.01688369E-03	1.50E-02	23830	2.65	464.0	1.0	3.73E-09	+
	IJAYA	2.42536062E-03	2.96867809E-03	2.52127917E-03	1.14E-04	30000	5.25	465.0	0.0	1.86E-09	+
	MLBSA	2.42507490E-03	3.27787002E-03	2.47513743E-03	1.54E-04	23724	8.08	397.0	38.0	2.43E-05	+
	TLABC	2.43288325E-03	2.38566346E+00	1.11964280E-01	4.53E-01	30000	14.08	465.0	0.0	1.86E-09	+
	PGJAYA	2.42529671E-03	2.58631693E-03	2.44895394E-03	3.18E-05	25286	3.11	452.0	13.0	1.64E-07	+
	ITLBO	2.42518618E-03	2.79774037E-03	2.46098942E-03	7.67E-05	19732	3.49	445.0	20.0	6.91E-07	+
	Rao-1	2.49047959E-03	3.73190068E-03	2.81845626E-03	2.64E-04	30000	2.18	465.0	0.0	1.86E-09	+
	ERao-1	**2.42507487E-03**	**2.43322333E-03**	**2.42556432E-03**	**1.50E-06**	8386	6.16				

ITLBO have excellent reliability on the SDM. For the DDM and TDM, only ERao-1 proposed in this paper can obtain the best RMSE result on Min, Max, Ave, and Std. While those who have achieved good results in SDM do not obtain the best result on the two models, which indicates that the proposed ERao-1 algorithm is still valid on the DDM and TDM. On the other hand, this also shows that with the increase of estimated unknown parameters, the performance of most algorithms has deteriorated. Besides, in view of the FEs, the proposed ERao-1 consumes the minimum FEs to find the optimal RMSE value for all models.

- From Table 10, it can be observed that ERao-1 and ITLBO achieve the best performance on the SDM in terms of the Min, Max, Mean, and Std, but ERao-1 only uses FEs = 4432 to find the best RMSE. For the DDM and TDM, ERao-1 achievs the best results on almost all indicators, except the CPU time.
- With respect of the Wilcoxon signed-ranks test results of the R.T.C France silicon and Photowatt-PWP201 cells, regardless of which models, it can be observed that ERao-1 performs better than GOTLBO, IJAYA, MLBSA, PGJAYA, Rao-1, while it is similar to ITLBO. In particular, for the DDM and TDM of Photowatt-PWP201 cell, ERao-1 significantly performs than its all competitors.
- As for the CPU time, it can be clearly seen that the original Rao-1 algorithm consumes the least time, while the proposed algorithm adds a certain amount of time. This is acceptable to a certain extent, because it has improved a lot in accuracy.

In addition, Figure 9 provides the Friedman test results on different PV models. It is worthwhile to mention that the smaller the average ranking of Friedman's test, the better the performance. From Figure 9, it can be seen that the average ranking of ERao-1 is significantly smaller than GOTLBO, IJAYA, MLBSA, TLABC, PGJAYA, and Rao-1 on the SDM, DDM, and TDM. Although the average

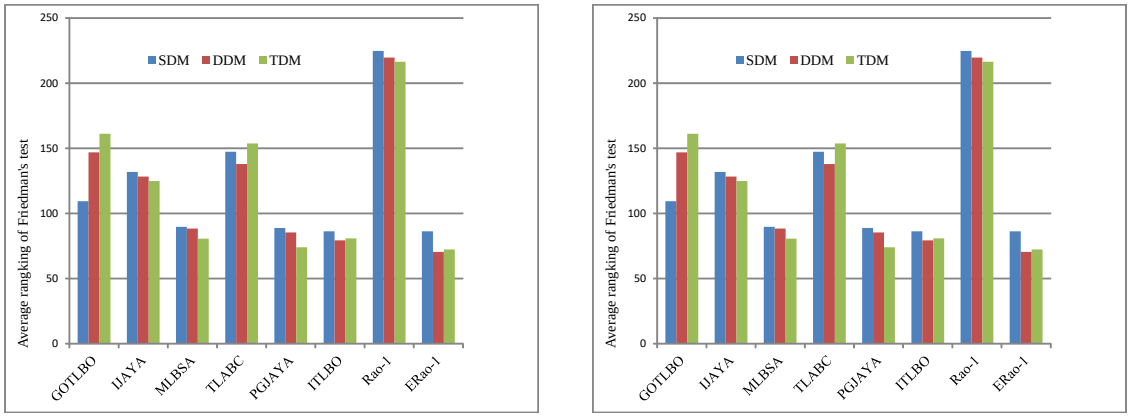

(a) R.T.C France silicon cell (b) Photowatt-PWP201 cell

Figure 9. Friedman test result of ERao-1 and compared algorithms on different PV models.

ranking of ITLBO and ERao-1 is not obvious on the SDM, ERao-1's average ranking is significantly smaller than ITLBO's on the DDM and TDM. Finally, Figure 10 plots the convergence curves of ERao-1 and its competitors, where it can be seen that ERao-1 has a faster convergence speed for the SDM, DDM and TDM of the R.T.C France silicon cell. In particular, for the DDM, IJAYA, GOTLBO, and MLBSA have a quick convergence in the early stage, but ERao-1 converges significantly faster to the optimum value after $FEs = 10000$. While for the Photowatt-PWP201 cell, ERao-1 obviously converges quickly on the SDM. Note that although ERao-1 in the other two models converges slower than its comparators in the early stage, it can be clearly seen that in the later stage, ERao-1 can converge to a more accurate RMSE value.

5.4. Compared with other reported results

In this section, the results of ERao-1 have been compared with some recent works such as enhanced Lévy flight bat algorithm (ELBA) [39], classified perturbation mutation PSO (CPMPSO) [40], niche-based PSO with parallel computing (NPSOPC) [41], improved equilibrium optimizer (IEO) [42], enhanced JAYA (EJAYA) [43], enhanced adaptive butterfly optimization algorithm (EABOA) [44], shuffled frog leaping with memory pool (SFLBS) [45], modified teachingClearning based optimization (MTLBO) [46], novel hybrid differential evolution and artificial bee colony (nDEBCO) [47], modified Rao-1 (MRao-1) [25], comprehensive learning JAYA (CLJAYA) [48], backtracking search algorithm with competitive learning (CBSA) [49]. The comparison result is given in Tables 11, 12, 13. Note that since there are too few studies on TDM of the R.T.C France silicon cell, and DDM, TDM of the Photowatt-PWP201 cell, we have not compared these results here. From these tables, it can observe that:

- For the SDM, almost all compared algorithms can provide the best RMSE (9.8602E-04), except the NPSOPC. While only EJAYA and proposed ERao-1 consume the least FEs to obtain the best solution.
- In terms of the DDM, it can be seen that most of the algorithms proposed in 2021 can obtain the best results. However, with the allowed maximum FEs consideration, it is evident that only

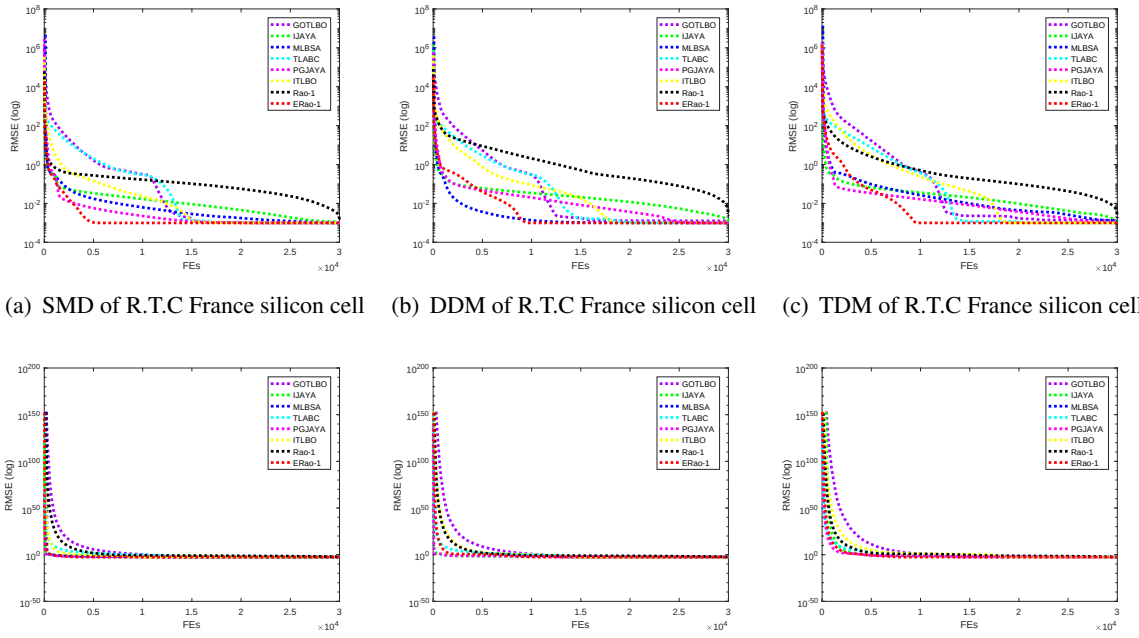

(a) SMD of R.T.C France silicon cell (b) DDM of R.T.C France silicon cell (c) TDM of R.T.C France silicon cell

(d) SDM of Photowatt-PWP201 cell (e) DDM of Photowatt-PWP201 cell (f) TDM of Photowatt-PWP201 cell

Figure 10. Convergence curves of ERao-1 and compared algorithms on different PV models.

ERao-1 uses the least FEs 30000, while 50000 for MRao-1, nDEBCO, and MTLBO.

- With respect to the single PVM of the Photowatt-PWP201, similar to the SDM, except for EABOA, other algorithms can obtain the optimal RMSE (2.4251E-03). CLJAYA, EJAYA, and ERao-1 consume the least FEs, while IEO is up to 1500000.

In summary, the proposed ERao-1 can not only obtain a comparable optimal solution when compared these well-established parameter estimation algorithms, but also uses the least FEs.

Table 11. Results of ERao-1 compared with other reported results on the SDM of the R.T.C France silicon cell.

Algorithm	I_{pg} (A)	I_{rs} (μA)	R_{se} (Ω)	R_{sh} (Ω)	n	RMSE	FEs
ELBA (2020) [39]	0.760776	0.323021	0.036377	53.718523	1.481185	9.8602E-04	50000
CPMPSO (2020) [40]	0.760776	0.323021	0.036377	53.71852	1.481184	9.8602E-04	50000
NPSOPC (2020) [41]	0.7608	0.3325	0.03639	53.7583	1.4814	9.8856E-04	NA
IEO (2020) [42]	0.760775529	0.323	0.036377	53.71852	1.481183	9.8602E-04	1500000
EJAYA (2021) [43]	0.76078	0.32302	0.03638	53.71852	1.48118	**9.8602E-04**	**30000**
EABOA (2021) [44]	0.760771077	0.322929	0.036379593	53.76600144	1.481153457	9.8602E-04	50000
SFLBS (2021) [45]	0.76078	0.323021	0.03638	53.7185	1.481184	9.8602E-04	60000
MTLBO (2021) [46]	0.76077553	0.323	0.03637709	53.7185251	1.48118359	9.8602E-04	50000
nDEBCO(2021) [47]	0.76077553	0.323020774	0.036377093	53.71852061	1.481180682	9.8602E-04	50000
MRao-1(2021) [25]	0.760776	0.323021	0.036377	53.718522	1.481135	9.8602E-04	50000
ERao-1	0.7608	0.3230	0.0364	53.7185	1.4812	**9.8602E-04**	**30000**

6. Conclusions

Aiming at the shortcomings of the original Rao-1 algorithm, this paper designs an enhanced Rao-1 algorithm short for ERao-1, to accurately and reliably estimate the unknown parameters in PV models.

Table 12. Results of ERao-1 compared with other reported results on the DDM of the R.T.C France silicon cell.

Algorithm	I_{pg} (A)	I_{rs1} (μA)	R_{se}	R_{sh} (Ω)	n_1	I_{rs2} (μA)	n_2	RMSE	FEs
ELBA (2020) [39]	0.760781	0.749338	0.03674	55.48544	2	0.225975	1.451018	9.8248E-04	50000
CLJAYA (2020) [48]	0.76078	0.226051	0.03674	55.48599	1.45105	0.74876	1.99999	9.8249E-04	48000
CPMPSO (2020) [40]	0.76078	0.74935	0.03674	55.48544	2	0.22597	1.45102	9.8248E-04	50,000
IEO (2020) [42]	0.760781	0.749	0.03674	55.48544	1.451016	0.226	1.999999	9.8248E-04	1500000
EABOA (2021) [44]	0.76082865	0.25072	0.0366266	55.3660129	1.45988481	0.72069	1.99997318	9.8607E-04	50000
SFLBS (2021) [45]	0.76077	0.775995	0.036755	55.5496	2		1.449857	9.8249E-04	60000
MTLBO (2021) [46]	0.760781	0.7493	0.03674043	55.485447	1.9999999	0.22597	1.451016	9.8248E-04	50000
nDEBCO(2021) [47]	0.760781079	0.749359716	0.036740432	55.48545905	1.451013864	0.22597418	2	9.8248E-04	50000
MRao-1(2021) [25]	0.760781	0.225959	0.03674	55.486045	1.450963	0.749667	2	9.8248E-04	50000
ERao-1	0.7608	0.7493	0.0367	55.4854	2.0000	0.2260	1.4510	**9.8248E-04**	**30000**

Table 13. Results of ERao-1 compared with other reported results on the single PVM of the Photowatt-PWP201 cell.

Algorithm	I_{pg} (A)	I_{rs} (μA)	R_{se} (Ω)	R_{sh} (Ω)	n	RMSE	FEs
CLJAYA (2020) [48]	1.030514	3.4822628	1.201271	981.982279	48.64283	**2.4251E-03**	**30000**
CBSA (2020) [49]	1.0275389	4.747459	1.340999	1087.81738	49.927517	2.4251E-03	25000
IEO (2020) [42]	1.030514254	3.48	1.201269	981.9956	48.64292	2.4251E-03	1500000
EJAYA (2021) [43]	1.03051	3.48226	1.20127	981.98235	48.64283	**2.4251E-03**	**30000**
EABOA (2021) [44]	1.03044416	3.5084	1.200630203	991.9830745	48.67132719	2.4252E-03	50000
SFLBS (2021) [45]	1.030514	3.48226	1.201271	981.9804	48.6428	2.4251E-03	60000
MTLBO (2021) [46]	1.0305143	3.4823	1.201271	981.9823732	48.6428349	2.4251E-03	50000
MRao-1(2021) [25]	1.030514	3.4823	1.201271	981.9821	48.64131	2.4251E-03	50000
ERao-1	1.0305	3.4823	1.2013	981.9822	48.6428	**2.4251E-03**	**30000**

In ERao-1, there are three main improvement points. First, a repaired evolution operator is presented to reduce the randomness of the original operator. Second, a new evolution operator is proposed to make full use of the population information and avoid the algorithm falling into a local optimum. Third, to make population size adaptively adjust, a population size linear reduction strategy is employed. ERao-1 is evaluated by estimating the unknown parameters of three different PV models. Experimental results demonstrate that the enhanced Rao-1 algorithm not only can achieve the best RMSE values (9.8602E-04 and 2.4251E-03) for the SDM, but also obtains the best result (9.8248E-04) for the DDM while its competitors can not achieve. In addition, the statistical results also prove the competitive performance of ERao-1 on the standard deviation and the consumed function evaluations to reach the optimal RMSE. Moreovr, two non-parametric statistical tests and the convergence curves also illustrate the superiority of proposed ERao-1 algorithm. Although the ERao-1 is not significantly optimal in terms of CPU time, it is acceptable to sacrifice less time to obtain more accurate solutions. Finally, it is worth noting that ERao-1 is only suitable for solving single-objective unconstrained optimization problems. If there are constraints, it needs to introduce constraint handle technology.

In future works, ERao-1 will be adopted to solve more complex optimization problems such as maximum power point tracking in PV system [50], optimal power flow in power system [51, 52], non-linear equation optimization problem [53], and so on.

Acknowledgments

This work was partly supported by the Hainan Provincial Natural Science Foundation of China under Grant No. 621RC599 and the National Natural Science Foundation of China under Grant No. 62076225.

Conflict of interest

The authors declare there is no conflict of interest.

References

1. S. Li, W. Gong, Q. Gu, A comprehensive survey on meta-heuristic algorithms for parameter extraction of photovoltaic models, *Renew. Sustain. Energy Rev.*, **141** (2021), 110828. doi: 10.1016/j.rser.2021.110828.
2. G. Xiong, J. Zhang, D. Shi, Y. He, Parameter extraction of solar photovoltaic models using an improved whale optimization algorithm, *Energy Convers. Manage.*, **174** (2018), 388–405. doi: 10.1016/j.enconman.2018.08.053.
3. T. Ayodele, A. Ogunjuyigbe, E. Ekoh, Evaluation of numerical algorithms used in extracting the parameters of a single-diode photovoltaic model, *Sustain. Energy Technol. Assess*, **13** (2016), 51–59. doi: 10.1016/j.seta.2015.11.003.
4. T. Babu, J. Ram, K. Sangeetha, A. Laudani, N. Rajasekar, Parameter extraction of two diode solar pv model using fireworks algorithm, *Sol. Energy*, **140** (2016), 265–276. doi: 10.1016/j.solener.2016.10.044.
5. S. Li, W. Gong, X. Yan, C. Hu, D. Bai, L. Wang, Parameter estimation of photovoltaic models with memetic adaptive differential evolution, *Sol. Energy*, **190** (2019), 465–474. doi: 10.1016/j.solener.2019.08.022.
6. T. Easwarakhanthan, J. Bottin, I. Bouhouch, C. Boutrit, Nonlinear minimization algorithm for determining the solar cell parameters with microcomputers, *Int. J. Sol. Energy*, **4** (1986), 1–12. doi: 10.1080/01425918608909835.
7. A. Conde, F. Sánchez, J. Muci, New method to extract the model parameters of solar cells from the explicit analytic solutions of their illuminated characteristics, *Sol. Energy Mater. Sol. Cells*, **90** (2006), 352–361. doi: 10.1016/j.solmat.2005.04.023.
8. R. Messaoud, Extraction of uncertain parameters of single-diode model of a photovoltaic panel using simulated annealing optimization, *Energy Rep.*, **6** (2020), 350–357. doi: 10.1016/j.egyr.2020.01.016.
9. M. AlHajri, K. Naggar, M. AlRashidi, A. Othman, Optimal extraction of solar cell parameters using pattern search, *Renew. Energy*, **44** (2012), 238–245. doi: 10.1016/j.renene.2012.01.082.
10. S. Ebrahimi, E. Salahshour, M. Malekzadeh, F. Gordillo, Parameters identification of pv solar cells and modules using flexible particle swarm optimization algorithm, *Energy*, **179** (2019), 358–372. doi: 10.1016/j.energy.2019.04.218.
11. S. Li, Q. Gu, W. Gong, B. Ning, An enhanced adaptive differential evolution algorithm for parameter extraction of photovoltaic models, *Energy Convers. Manage.*, **205** (2020), 112443. doi: 10.1016/j.enconman.2019.112443.
12. Z. Yan, S. Li, W. Gong, An adaptive differential evolution with decomposition for photovoltaic parameter extraction, *Math. Biosci. Eng.*, **18** (2021), 7363–7388. doi: 10.3934/mbe.2021364.

13. S. Li, W. Gong, L. Wang, X. Yan, C. Hu, A hybrid adaptive teaching-learning-based optimization and differential evolution for parameter identification of photovoltaic models, *Energy Convers. Manage.*, **225** (2020), 113474. doi: 10.1016/j.enconman.2020.113474.

14. D. Oliva, M. Aziz, A. Hassanien, Parameter estimation of photovoltaic cells using an improved chaotic whale optimization algorithm, *Appl. Energy*, **200** (2017), 141–154. doi: 10.1016/j.apenergy.2017.05.029.

15. X. Chen, K. Yu, W. Du, W. Zhao, G. Liu, Parameters identification of solar cell models using generalized oppositional teaching learning based optimization, *Energy*, **99** (2016), 170–180. doi: 10.1016/j.energy.2016.01.052.

16. K. Yu, J. Liang, B. Qu, X. Chen, H. Wang, Parameters identification of photovoltaic models using an improved jaya optimization algorithm, *Energy Convers. Manage.*, **150** (2017), 742–753. doi: 10.1016/j.enconman.2017.08.063.

17. K. Yu, J. Liang, B. Qu, Z. Cheng, H. Wang, Multiple learning backtracking search algorithm for estimating parameters of photovoltaic models, *Appl. Energy*, **226** (2018), 408–422. doi: 10.1016/j.apenergy.2018.06.010.

18. X. Chen, B. Xu, C. Mei, Y. Ding, K. Li, Teaching-learning-based artificial bee colony for solar photovoltaic parameter estimation, *Appl. Energy*, **212** (2018), 1578–1588. doi: 10.1016/j.apenergy.2017.12.115.

19. K. Yu, B. Qu, C. Yue, S. Ge, X. Chen, J. Liang, A performance-guided jaya algorithm for parameters identification of photovoltaic cell and module, *Appl. Energy*, **237** (2019), 241–257. doi: 10.1016/j.apenergy.2019.01.008.

20. S. Li, W. Gong, X. Yan, C. Hu, D. Bai, L. Wang, et al., Parameter extraction of photovoltaic models using an improved teaching-learning-based optimization, *Energy Convers. Manage.*, **186** (2019), 293–305. doi: 10.1016/j.enconman.2019.02.048.

21. R. Rao, Rao algorithms: three metaphor-less simple algorithms for solving optimization problems, *Int. J. Ind. Eng. Comput.*, **11** (2020), 107–130. doi: 10.5267/j.ijiec.2019.6.002.

22. R. Rao, R. Pawar, Constrained design optimization of selected mechanical system components using rao algorithms, *Appl. Soft Comput.*, **89** (2020), 106141. doi: 10.1016/j.asoc.2020.106141.

23. M. Srikanth, N. Yadaiah, Analytical tuning rules for reduced-order active disturbance rejection control with fopdt models through multi-objective optimization and multi-criteria decision-making, *ISA Trans.*, **114** (2021), 370–398. doi: 10.1016/j.isatra.2020.12.035.

24. L. Wang, Z. Wang, H. Liang, C. Huang, Parameter estimation of photovoltaic cell model with rao-1 algorithm, *Optik*, **210** (2020), 163846. doi: 10.1016/j.ijleo.2019.163846.

25. X. Jian, Y. Zhu, Parameters identification of photovoltaic models using modified rao-1 optimization algorithm, *Optik*, **231** (2021), 166439. doi: 10.1016/j.ijleo.2021.166439.

26. M. Alrashidi, M. Alhajri, K. Elnaggar, A. Alothman, A new estimation approach for determining the i-v characteristics of solar cells, *Sol. Energy*, **85** (2011), 1543–1550. doi: 10.1016/j.solener.2011.04.013.

27. K. Naggar, M. AlRashidi, M. AlHajri, A. Othman, Simulated annealing algorithm for photovoltaic parameters identification, *Sol. Energy*, **86** (2012), 266–274. doi: 10.1016/j.solener.2011.09.032.

28. A. Askarzadeh, A. Rezazadeh, Parameter identification for solar cell models using harmony search-based algorithms, *Sol. Energy*, **86** (2012), 3241–3249. doi: 10.1016/j.solener.2012.08.018.

29. W. Huang, C. Jiang, L. Xue, D. Song, Extracting solar cell model parameters based on chaos particle swarm algorithm, In *2011 International Conference on Electric Information and Control Engineering*, pages 398–402, April 2011. doi: 10.1109/ICEICE.2011.5777246.

30. K. Ishaque, Z. Salam, S. Mekhilef, A. Shamsudin, Parameter extraction of solar photovoltaic modules using penalty-based differential evolution, *Appl. Energy*, **99** (2012), 297–308. doi: 10.1016/j.apenergy.2012.05.017.

31. H. Hasanien, Shuffled frog leaping algorithm for photovoltaic model identification, *IEEE Trans. Sustain. Energy*, **6** (2015), 509–515. doi: 10.1109/TSTE.2015.2389858.

32. J. Ram, T. Babu, T. Dragicevic, N. Rajasekar, A new hybrid bee pollinator flower pollination algorithm for solar pv parameter estimation, *Energy Convers. Manage.*, **135** (2017), 463–476. doi: 10.1016/j.enconman.2016.12.082.

33. K. Yu, X. Chen, X. Wang, Z. Wang, Parameters identification of photovoltaic models using self-adaptive teaching-learning-based optimization, *Energy Convers. Manage.*, **145** (2017), 233–246. doi: 10.1016/j.enconman.2017.04.054.

34. F. Zeng, H. Shu, J. Wang, Y. Chen, B. Yang, Parameter identification of pv cell via adaptive compass search algorithm, *Energy Rep.*, **7** (2021), 275–282. doi: 10.1016/j.egyr.2021.01.069.

35. G. Xiong, L. Li, A. Mohamed, X. Yuan, J. Zhang, A new method for parameter extraction of solar photovoltaic models using gaining sharing knowledge based algorithm, *Energy Rep.*, **7** (2021), 3286–3301. doi: 10.1016/j.egyr.2021.05.030.

36. W. Li, W. Gong, Differential evolution with quasi-reflection-based mutation, *Math. Biosci. Eng.*, **18** (2021), 2425–2441. doi: 10.3934/MBE.2021123.

37. Q. Pang, X. Mi, J. Sun, H. Qin, Solving nonlinear equation systems via clustering-based adaptive speciation differential evolution, *Math. Biosci. Eng.*, **18** (2021), 6034–6065. doi: 10.3934/MBE.2021302.

38. S. García, D. Molina, M. Lozano, F. Herrera, A study on the use of non-parametric tests for analyzing the evolutionary algorithms behaviour: a case study on the cec 2005 special session on real parameter optimization, *J. Heurist.*, **15** (2009), 617–644. doi: 10.1007/s10732-008-9080-4.

39. L. Deotti, J. Pereira, I. Jénior, Parameter extraction of photovoltaic models using an enhanced lévy flight bat algorithm, *Energy Convers. Manage.*, **221** (2020), 113114. doi: 10.1016/j.enconman.2020.113114.

40. J. Liang, S. Ge, B. Qu, K. Yu, F. Liu, H. Yang, et al., Classified perturbation mutation based particle swarm optimization algorithm for parameters extraction of photovoltaic models, *Energy Convers. Manage.*, **203** (2020), 112138. doi: 10.1016/j.enconman.2019.112138.

41. X. Lin, Y. Wu, Parameters identification of photovoltaic models using niche-based particle swarm optimization in parallel computing architecture, *Energy*, **196** (2020), 117054. doi: 10.1016/j.energy.2020.117054.

42. M. Basset, R. Mohamed, S. Mirjalili, R. Chakrabortty, M. Ryan, Solar photovoltaic parameter estimation using an improved equilibrium optimizer, *Sol. Energy*, **209** (2020), 694–708. doi: 10.1016/j.solener.2020.09.032.
43. X. Yang, W. Gong, Opposition-based jaya with population reduction for parameter estimation of photovoltaic solar cells and modules, *Appl. Soft Comput.*, **104** (2021), 107218. doi: 10.1016/j.asoc.2021.107218.
44. W. Long, T. Wu, M. Xu, M. Tang, S. Cai, Parameters identification of photovoltaic models by using an enhanced adaptive butterfly optimization algorithm, *Energy*, **229** (2021), 120750. doi: 10.1016/j.energy.2021.120750.
45. Y. Liu, A. Heidari, X. Ye, C. Chi, X. Zhao, C. Ma, et al., Evolutionary shuffled frog leaping with memory pool for parameter optimization, *Energy Rep.*, **7** (2021), 584–606. doi: 10.1016/j.egyr.2021.01.001.
46. M. Basset, R. Mohamed, R. Chakrabortty, K. Sallam, M. Ryan, An efficient teaching-learning-based optimization algorithm for parameters identification of photovoltaic models: Analysis and validations, *Energy Convers. Manage.*, **227** (2021), 113614. doi: 10.1016/j.enconman.2020.113614.
47. O. Hachana, B. Aoufi, G. Tina, M. Sid, Photovoltaic mono and bifacial module/string electrical model parameters identification and validation based on a new differential evolution bee colony optimizer, *Energy Convers. Manage.*, **248** (2021), 114667. doi: 10.1016/j.enconman.2021.114667.
48. Y. Zhang, M. Ma, Z. Jin, Comprehensive learning jaya algorithm for parameter extraction of photovoltaic models, *Energy*, **211** (2020), 118644. doi: 10.1016/j.energy.2020.118644.
49. Y. Zhang, M. Ma, Z. Jin, Backtracking search algorithm with competitive learning for identification of unknown parameters of photovoltaic systems, *Expert Syst. Appl.*, **160** (2020), 113750. doi: 10.1016/j.eswa.2020.113750.
50. L. Tang, X. Wang, W. Xu, C. Mu, B. Zhao, Maximum power point tracking strategy for photovoltaic system based on fuzzy information diffusion under partial shading conditions, *Sol. Energy*, **220** (2021), 523–534. doi: 10.1016/j.solener.2021.03.047.
51. S. Li, W. Gong, L. Wang, X. Yan, C. Hu, Optimal power flow by means of improved adaptive differential evolution, *Energy*, **198** (2020), 117314. doi: 10.1016/j.energy.2020.117314.
52. S. Li, W. Gong, C. Hu, X. Yan, L. Wang, Q. Gu, Adaptive constraint differential evolution for optimal power flow, *Energy*, **235** (2021), 121362. doi: 10.1016/j.energy.2021.121362.
53. W. Gong, Z. Liao, X. Mi, L. Wang, Y. Guo, Nonlinear equations solving with intelligent optimization algorithms: a survey, *Complex Syst. Model. Simul.*, **1** (2021), 15–32. doi: 10.23919/CSMS.2021.0002.

AIMS Press